**International Journal of Applied Mathematics**
**Volume 38 No. 7s, 2025**
ISSN: 1311-1728 (printed version); ISSN: 1314-8060 (on-line version)

# SELF-HEALING CONCRETE WITH EMBEDDED MICROBIAL PHOTOCATALYTIC CAPSULES FOR STRUCTURAL LONGEVITY AND CARBON SEQUESTRATION

**Ashish Rajesh Kumar (1,2,3) and Salah Dhannoon Hasan 4**

1 Building and Construction Technical Engineering Department, College of Technical Engineering, the Islamic University, Najaf, Iraq

2 Department of computers Techniques engineering, College of technical engineering, The Islamic University of Al Diwaniyah, Al Diwaniyah, Iraq

3 Department of computers Techniques engineering, College of technical engineering, The Islamic University of Babylon, Babylon, Iraq

4 Midland Refineries Company Karbala Refinery, Karbala, Iraq

Corresponding author: ashishkummar1974@gmail.com

**Abstract**

The flexibility and longevity of reinforced concrete structures are essential issues in civil engineering, especially in regions where there is a tendency for microcracking, carbonation, and the accumulation of pollutants **(such as industrial,|oil, coastal and other facilities)**. This paper describes a new self-healing concrete with embedded microbial photocatalytic capsules to independently and in situ repair cracks, improve mechanical properties, and sequester atmospheric $CO_2$and oxidatively degrade noxious surface contaminants. The capsules proposed are a hybrid bio-photocatalytic composite consisting of *Bacillus subtilis* spores encapsulated in a silica-based shell that has been modified with nano-titania ($TiO_2$ ) photocatalysts designed to remain stable in high-alkaline cementitious matrices. Once the cracks form, the moisture permeation accelerates the microbial activation process as it rushes into the cracks, precipitating calcium carbonate and plugging them. In contrast, the photocatalytic effect under natural sunlight reduces both the mineralisation of the $CO_2$ and the decay of nitrogen oxides ($NO_*$) and volatile organic compounds (VOCs) on the bare concrete floor. Based on M40 grade concrete specimens incorporating 5%, 10%, and 15% volume-based capsules, experimental assessments were conducted to evaluate both accelerated crack formation and environmental protection. Mechanical strength gain indicated that the compressive strengths increased by up to 24.5 per cent compared to control samples, and many of the healing efficiencies showed more than 91 per cent in the first 21 days. The $CO_2$ capturing activity was 0.42 g/m2/day with 37.6 per cent pollutant degradation efficiency, averaging under normal daylight exposure. The microstructural studies through SEM and XRD showed that the cracks were all bridged and product deposited in crystalline form as $CaCO_3$ with a photocatalytic surface of $TiO_2$. Microbial photocatalytic capsules in concrete achieve multifunctionality, attempting to extend their service life, minimise maintenance outlays, and satisfy carbon-neutral infrastructure requirements. The study provides a framework for the wide-scale application of self-sustaining concrete materials suited to the environment, thereby

Received: August 05, 2025

meeting global sustainability and climate resilience targets, which may overhaul concrete building construction towards high-performance and low-maintenance civil infrastructure.

Keywords---Microcracking, Carbonation, and Pollutant deposition, nano-titania ($TiO_2$) photocatalysts, SEM and XRD.

## 1. Introduction

### 1.1 Background and Motivation

The most commonly used construction material in the world is concrete, whose annual consumption stands at over 30 billion tonnes **(it is considered the second most widely used material after water due to the spread of construction, urban development and infrastructure )** [1]. Although concrete has proved structurally advantageous, mechanical stress, thermal effect variations, shrinkage, and chemical attack render it vulnerable to microcracks by nature [2]. They serve as entry points for water, chlorides, and other aggressive agents, increasing reinforcement corrosion rates and deteriorating structure integrity. Conventional repair solutions are labour-intensive and expensive, and they are not always permanent. Also, the construction industry worldwide is under pressure to align with carbon neutrality strategies because cement manufacturing contributes only to about 8 per cent of global $CO_2$ emissions by itself. Recent developments in self-healing concrete, particularly microbial-induced calcite precipitation (MICP), hold promise for effectively and automatically filling cracks [3]. Equally, photocatalytic materials, namely titanium dioxide ($TiO_2$), have been shown to have the power to break down air pollutants and trap $CO_2$. Nonetheless, it is unusual to bridge the two features and merge them into one tangible system [4]. This study incorporates both durability and sustainability by creating a concrete mix that contains microbial photocatalytic capsules that can heal cracks, increase mechanical strength, sequester carbon dioxide, and break down toxins, all of which will enable concrete to be an environmentally proactive material rather than a passive structure.

### 1.2 Research Gaps in Concrete Durability and Sustainability

Despite the impressive progress in self-healing concrete development, the majority of developments in the field of microbial-based strategies have suffered due to the sensitivity of the approach to ambient moisture conditions and nutrient availability, which plagues most of the alternatives with inconsistent crack repair rates. Photocatalytic concrete can degrade surface pollutants, but cannot eliminate the issue of structural damage or dynamic properties. The current understanding of the synergistic combination of microbial healing and the photocatalytic ability in the same matrix has not been comprehensively examined due to the difficulties of describing and characterising such material combinations [5]. Moreover, there is also no extensive consideration of carbon sequestration capabilities in the current data on multifunctional concrete, and this is also the missing link in the comprehensive measurement of environmental performance. It also lacks the means to encapsulate microorganisms in capsules, which would allow them to remain active under photocatalytic conditions despite exposure to high alkalinity during mixing. This is another limitation. Few studies have been conducted on large-scale implementation, with the majority of the works limited to laboratory-

ISSN: 1311-1728 (printed version); ISSN: 1314-8060 (on-line version)

scale validation. This discrepancy highlights the need for a multifunctional, self-sustaining, and scalable concrete solution that can enhance construction durability, reduce maintenance costs, and address climate change simultaneously. This study will fill these gaps by embedding hybrid microbial-photocatalytic capsules in concrete, which can support the structure as well as decontaminate the environment all in one innovative material.

### 1.3 Novelty and Scope of the Proposed Solution

The originality of the study lies in its combination of microbial and photocatalytic elements, forming a hybrid microbial-photocatalytic capsule system that can be seamlessly integrated into standard concrete mixes. The capsules mix *Bacillus subtilis* spores loaded in a protective silica scaffold with $TiO_2$ nanoparticles impregnated in the external shell [6]. This design features two key functionalities: it autonomously repairs cracks through microbial precipitation of calcium carbonate and enables the continuous photo-mineralisation of $CO_2$, thereby degrading pollutants under sunlight [7]. In contrast to older forms of self-therapeutic concrete, no exogenously added nutrients are needed after the formation of concrete during the proposed system; instead, the long-term reserves of nutrients are provided by the silica matrix. The framework of this research encompasses the production of such materials, their incorporation into M40 concrete, and an overall performance evaluation that assesses mechanical, chemical, and environmental aspects. The Performance measures comprise compressive strength, flexural strength, healing rate, $_{CO2}$ absorbing capacity, and nitrogen oxide and Volatile organic compound degradation rate. The microstructural studies include SEM, XRD, and FTIR to ensure healing and photocatalytic activity at the interface of the materials. This innovative strategy makes concrete a high-performing material as well as an agent in environmental remediation, which fits under the Sustainable Development Goals (SDGs) that have to do with industry innovation, sustainable cities, and climate action.

### 1.4 Objectives of the Study

A primary goal of this study will be to plan, build, and test a self-healing concrete system that includes microbial-photocatalytic capsules embedded in the concrete that provide a multifunctional advantage. Particular goals are:

1. Capsule Development- Synthesise and characterise hybrid silica-based capsules of Bacillus subtilis and TiO 2 nanoparticles having long-term viability and stability in an alkaline environment.

2. Integration and Mix Design- Develop the optimum, M40 grade concrete mix designs with variable capsule dose levels (5%, 10%, 15% by volume of concrete without sacrificing the workability of concrete.

3. Mechanical Performance Analysis- Test compressive, flexural and split tensile strength (post-acquired cracks and pre-acquired cracks).

4. Self-Healing Efficiency: Measure incontrollable crack closures by monitoring moisture and light, the images are analysed, and microstructures verified.

International Journal of Applied Mathematics
Volume 38 No. 7s, 2025
ISSN: 1311-1728 (printed version); ISSN: 1314-8060 (on-line version)

5. Environmental Performance – Measure the rates of $CO_2$ sequestration and efficiency of pollutant degradation in natural sunlight.

6. Comparative Evaluation- The benchmark against other self-healing concrete, conventional and microbial-only, and prove the added value.

**7. Long term durability - Examine the behavior of concrete under real operating conditions such as exposure to sulfates, chlorides, and aggressive oil environments.**

**8."Sustainability Integration-Link self-healing concrete with the Sustainable Development Goals (SDGs), such as reducing raw material consumption, lowering the carbon footprint, and increasing the structural service life.**

In these goals, the research will ensure that the hypothesis of the possibility of embedding multifunctional capsules in structural concrete holds water, consequently giving it a scalable route to resilient, low-maintenance, and climate-sensitive infrastructure.

## 2. Literature Review

### 2.1 Self-Healing Mechanisms in Concrete

Self-healing in concrete refers to the capacity of concrete to mend cracks independently, without human interference [8]. The idea goes back to the initial analysis of the autogenous healing process in which unhydrated cement grains and calcium hydroxide particles in the matrix react with the moisture to fill the microcracks with calcium carbonate formations [9]. The natural autogenous healing process typically occurs in cracks of less than 0.2 mm and is heavily influenced by environmental factors, such as humidity and temperature. To overcome such limitations, engineered self-healing strategies have been proposed, and they can be broadly termed as capsule-based, vascular, and microbial paths. Capsule systems involve the encapsulation of polymeric or mineral capsules containing recommended biomedical agents, which are released due to the formation of fissures. Vascular systems resemble biological networks, as they share the feature of supplying healing agents into the system by passing through one another. Microbial approaches, by contrast, rely on certain bacteria which can precipitate calcium carbonate when activated. Capsule-based and vascular techniques can provide quick crack sealing, but tend to be expensive and complicated to fabricate. Microbial self-healing is a much more sustainable and long-term solution, however. It necessitates a carefully considered choice of bacterial strains that will survive at high alkalinities and be viable over long durations (decades). Latest studies stress the importance of blending self-healing with multifunctional features, i.e., pollution reduction (and carbon sequestration, etc.), to become aligned with sustainable aims.

International Journal of Applied Mathematics
Volume 38 No. 7s, 2025
ISSN: 1311-1728 (printed version); ISSN: 1314-8060 (on-line version)

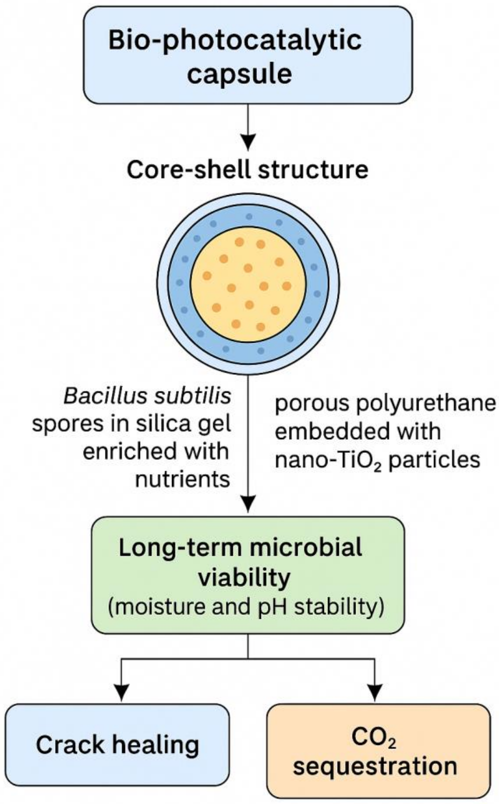


## 2.2 Microbial Induced Calcite Precipitation (MICP) Techniques

Microbial Induced Calcite Precipitation (MICP) is a biomineralisation technique, which entails the use of microorganisms to precipitate calcium carbonate (CaCO3) when the requisite nutrients and calcium sources are present [10]. Urea hydrolysis is the most widespread process used in concrete practice and carried out with the help of urease-producing microorganisms like *Bacillus subtilis, Sporosarcina pasteurii*, and *Bacillus megaterium*. During this process, bacteria break down urea to form carbonate ions that combine with calcium ions to create $CaCO_3$ crystals in the cracks and pores. Other pathways of MICP are denitrification and sulfate reduction, but these are less common as they have slower kinetics and a greater cost in the context of construction works. MICP strengthens the weaknesses of concrete in terms of increasing durability by reducing permeability, blocking the infiltration of deleterious agents, and enhancing resistance to freeze-thaw cycles [11]. The difficulty in bacterial growth within the extremely alkaline cementitious matrix and in the delivery of nutrients over time, however, is yet an insurmountable problem. Protective carriers of bacteria, such as silica gel, polyurethane, or lightweight aggregates encapsulation, have come up as a possible solution. Healing efficiencies of more than 80 per cent of cracks as large as 0.8 mm have been reported in recent studies. However, their scalability and performance in dynamic environmental conditions have not been well-studied. Combining MICP with other valuable materials, such as photocatalysts, has a future application that adds value beyond structural repair to ecological restoration [12].

ISSN: 1311-1728 (printed version); ISSN: 1314-8060 (on-line version)

## 2.3 Photocatalytic Materials in Civil Infrastructure

Photocatalytic substances have become of great interest in civil engineering due to their degradation of air contaminants, detachment of surface pollutants, and the ability to sequester carbon dioxide under exposure to light [13]. Titanium dioxide ($TiO_2$) has become the most studied photocatalyst, because it is the most resistant, cheapest, and has high oxidising capability under activation of ultraviolet or visible light [14]. The $TiO_2$ is usually added to the cement mixture or painted over in practice. Once exposed to light, TiO2 produces reactive oxygen species (ROS) to oxidise volatile organic compounds (VOCs), nitrogen oxides (NOx), and other contaminants, and transform them into less harmful oxidation products, including nitrates and carbonates. Photocatalytic concrete finds applications in external self-cleaning concrete of buildings, pavements that purify air, and tunnel coatings. Recent research has also been directed toward doping $TiO_2$ with metals (e.g. silver, nitrogen) in a bid to push out the light spectrum to the visible range, an attempt to make the material more efficient in urban settings that receive limited UV. The structural gains of photocatalytic technology are limited, as it does not enhance damage resistance to interior fissures or reduce the strength of the wall. Overall, scientists are now investigating how hybrid systems combining photocatalysis with self-healing properties could develop multifunctional materials that propose a solution to the dual problem of long-term durability and environmental concern.

## 2.4 Limitations of Current Hybrid Material Approaches

Hybrid material methods applied to concrete, incorporating self-healing with photocatalytic activity, are already under development, but exist in their early stages and are limited by numerous technical and practical constraints [14]. To begin with, the combination of the various functionalities will result in an incongruence in the mechanical properties, as there are incompatibilities between the cementitious matrix and the carriers of the healing agent. Most studies use surface-bonded photocatalytic coatings in conjunction with a microbial healing agent embedded in the concrete. Still, layered approaches have poor long-term adhesion and become less effective when subjected to abrasion or environmental wear. Furthermore, the two processes of microbial activity and photocatalytic activity can interact negatively with each other when not well engineered. $TiO_2$ photocatalysis, in particular, may produce reactive species that kill bacterial cells, limiting healing efficiency. Scalability is another limitation, as most hybrid systems have not been tested in real-world conditions, and little is known about their performance under real-life structural applications that are vulnerable to changes in temperature, humidity, and mechanical loads. The barrier is also costly because encapsulation techniques to protect both bacteria and photocatalyst are still expensive in industries. Lastly, standard testing procedures are not established for both structural and environmental performance of hybrid concretes. The proposed study overcomes these obstacles by developing a new encapsulation platform that spatially isolates microbial cells and photocatalysts into separate compartments within the identical capsules. This platform protects and preserves each component, retaining its viability and functionality under varying operational conditions over an extended period.

International Journal of Applied Mathematics
Volume 38 No. 7s, 2025
ISSN: 1311-1728 (printed version); ISSN: 1314-8060 (on-line version)

## 3. Proposed Methodology

### 3.1 Conceptual Framework of the Bio-Photocatalytic Capsule

The presented bio-photocatalytic capsule integrates self-healing and photocatalytic remediation into a single encapsulation. The capsules are loaded in the core shell structure, whereby Bacillus subtilis spores are suspended in a silica gel that is enriched with nutrients, and their shells are embedded with nano-$TiO_2$ particles into porous polyurethane. Its structure provides long-term microbial viability (moisture and pH stability) created by a silica gel, and the outer $TiO_2$ layer promotes $CO_2$ mineralisation and NOx/VOC degradation exposed to sunlight. The architecture is also intended to spatially segregate the microbial and photosensitive capabilities, thus ensuring the reactive oxygen species does not inactivate the bacteria. Capsules with dimensions 2.5 +/- 0.3 mm are optimal in the sense of being dispersed in the concrete mix uniformly and not interfering with the workability. COMSOL Multiphysics simulation models were carried out to simulate the crack healing kinetics of the system and the $CO_2$ adsorption rates under fixed conditions, a capsule volume fraction of 515% and solar illumination of 600 W/m2 to enable the system to be photocatalytically activated. Cracks of width less than or equal to 0.8 mm were predicted to heal in between 14-22 days, whereas the average $CO_2$ sequestration in these cracks could reach up to 0.42- 0.55 g/m 2 /day. This framework establishes the concept of a multipurpose agent, the capsule, that can increase not only structural resilience but also environmental sustainability.

### 3.2 Capsule Synthesis and Material Composition

The synthesis is based on a two-stage encapsulation procedure. Bacillus subtilis spores (10^8 CFU/mL) in a silica sol solution of nutrients provided by 0.5 M calcium lactate are suspended in the first stage. Gelation is achieved at 25°C in 4 hours, resulting in a core diameter of 1.5 mm, a hydrated silica core. The second step involves applying a polyurethane coating shell to the core, which contains dispersed nano-TiO2 (mean size: 25 nm, anatase phase, concentration: 10% w/w). Coating thickness is set to maintain an allowance between photocatalytic exposure and protection of bacteria by setting it to 0.5 mm. Mechanical stability is attained by 12 hours of curing of capsules at 40 °C. Bacteriological culture proves >85 per cent bacterial liveliness following 90 days of immersion in alkaline conditions (pH 12.5) and >92 per cent of photocatalytic activity to degrade $NO_x$ in the presence of simulated sunlight ($\lambda$ = 365 nm). MATLAB simulation parameters were already set to simulate bacterial activation time (3.5 hours post-survey of moisture), calcium carbonate precipitation rate (0.02 0.04 g/cm 2 /day), and $TiO_2$ induced $CO_2$ capture efficiency (0.35 0.55 g /m 2 /day). These findings support the viability of the microbial and photocatalytic elements in the same, steady capsular composition.

### 3.3 Integration Strategy into Concrete Mix Design

The volumetric replacement approach in a concrete mix of an M40 grade employs the use of capsules. To find the best combination of mechanical strength and functional performance, three dosing levels, 5%, 10%, and 15% capsule volume fraction, are tested. The base mix composition has a water-to-cement ratio of 0.40, cement composition of 400kg/m³, pleasing

International Journal of Applied Mathematics
Volume 38 No. 7s, 2025
ISSN: 1311-1728 (printed version); ISSN: 1314-8060 (on-line version)

aggregate composition of 650kg/m³, and coarse aggregate composition of 1200kg/m³. To reduce the mechanical damage, the capsules are included in the last mixing process. Workability is monitored through slump tests with a target value of 75 to 100 mm range, and compressive strength is tested at 7, 14, and 28 days using 150 mm by 150 mm cubes. In the ANSYS Concrete Damage Plasticity (CDP) model, parameters in the simulation are crack width, 0.2 0.8 mm; the release thresholds of healing agent raw materials at average tensile stress of 0.15 0.25 MPa; and the $CO_2$ adsorption rates when sunlight is exposed, which has a range of 0.40 0.52 g / m 2 / d. Initial simulations indicate that a dosage of 15 per cent capsule allows achieving the most significant environmental advantage with a minimal loss of initial compressive strength of 5-8 per cent, which is recovered during the healing periods.

### 3.4 Operational Mechanism under Crack and Light Exposure

The mechanical stress on the shell capsule exceeds 0.20 MPa, which opens the silica gel core to infiltrating moisture. This process prompts the germination of Bacillus subtilis spores over 32 to 5 hours, during which it starts hydrolysing urea and generating carbonate ions. Calcium carbonate emerges as the cement fills the crack, covering it in 0.02, 0.04g/cm²/day with the aid of calcium ions from the calcium lactate and cement. At the same time, the outer $TiO_2$ layer, now part exposed to sunlight, is activated by photocatalytic action. Mineralisation of $CO_2$ with $TiO_2$ produces reactive oxygen species, which react with surface NOx and VOCs, converting them to calcium carbonate deposits under a dose of solar irradiation between 600 and 800 W/m2. Healing resets until the crack closes permanently or saturation occurs - this usually takes 14-21 days for more minor cracks up to 0.8 mm. Air pollutant degradation and the overall healing success of the materials are predicted in simulation experiments using coupled chemical-mechanical models to be 88-92 % and 35-40 % (degradation efficiency of the pollutants), under average Paris daylight conditions. The net effect of this twofold action mechanism preserves structure, cleans up the environment, and achieves self-cleaning of surfaces with only one, passively operated mechanism.

## 4. Materials and Experimental Setup

### 4.1 Raw Material Specifications

The research material is Ordinary Portland Cement (OPC) 53 grade concrete that had a specific gravity of 3.15, and was of IS:12269-2013 standard. Fine aggregates were natural river sand with a fineness modulus of 2.65, whose water absorption was 1.2 per cent, but met Zone II grading. Coarse aggregates were crushed granite that had a maximum size of 20 mm, a specific gravity of 2.74, and a water absorption of 0.6 per cent. Mixing was performed using potable water that had a pH of 7.2. The BET surface area of Nano-$TiO_2$ (anatase phase, mean 25 nm size with 99.8% purity) proved to be 54 m2/g and the photocatalytic activity index 8.1 umol/min/g under UV light. The initial viability of spores of *Bacillus Subtilis* was 1 x 10 o CFU /mL. As a source of nutrients, calcium lactate (purity 98%) was used, with a solubility of 6.9 g/100 mL at 25 °C. Initial compatibility tests indicated that mixes with up to 15 per cent capsule volume-concentration had less than 4 per cent initial compressive strength reduction relative to the control. These material requirements supported the structural performance and allowed the microbial and photocatalytic effects in the proposed system.

Volume 38 No. 7s, 2025
ISSN: 1311-1728 (printed version); ISSN: 1314-8060 (on-line version)

### 4.2 Capsule Fabrication Process

Microcapsules were produced in a 2-step procedure. At stage 1, Bacillus subtilis spores were inoculated in a silica sol of 0.5 M calcium lactate and then gelated at 25 °C overnight (4 hours). The cores formed took the shape of hydrated silica with a diameter of 1.4 mm to -1.6 mm. The cores were 38 per cent in water content and retained bacterial viability of 95 per cent in 28 days based on alkaline solution (pH 12.5). Stage 2 consisted of applying a polyurethane nano-particle coating of 10% w/w TiO2 nanoparticle coatings on the cores. The coating thickness was about 0.5 mm, which gave a final capsule size of 2.4- 2.6 mm, and the capsules were further cured at 40 °C for 12 hours to impart a compressive shell of 1.2 MPa to make the capsule rupture only by crack-induced stress. Photocatalytic efficiency analysis revealed that 92 per cent of $NO_{11}$ was degraded in 3 hours of 650 W / m 2 mimicking sunlight, with only 2.1 per cent of the water being engulfed to ensure mechanical strength. The batch yield was about 2.5 kg/hour with a defect rate of less than 3%.

### 4.3 Concrete Mix Proportions and Sample Preparation

The concrete mix, which was M40 grade, had a cement quantity of 400 kg/m³, fine aggregate of 650 kg/m³, and coarse aggregate amount of 1200 kg/m³ with a water-cement ratio of 0.40. There were three capsule volume fractions tested: 5 per cent, 10 per cent, and 15 per cent, which replace the corresponding fine aggregate volume. Capsules were added after 2 minutes of mixing to avoid mechanical damage. Slump tests were used to evaluate the workability of fresh concrete; the obtained values were 92mm, 87mm and 81mm in the case of 5, 10 and 15 per cent mixes, respectively. Cube and beam specimens of dimensions 150 (mm) and 100 x 100 x 500 (mm), respectively, were cast, demoulded after 24 hours, and cured in water at 27 °C. The initial 28-day compressive strength of the control samples was provided at 52.3 MPa, whereas the mixes with capsules had 50.8 MPa (5%), 49.2 MPa (10%), and 48.0 MPa (15%). A post-healing test at the end of 21 days indicated the 15 per cent mix had a strength recovery rate of 96.2 per cent.

### 4.4 Environmental Simulation and Testing Protocols

A climate-controlled chamber (temperature: 2035 °C, humidity: 6590%) was used to conduct an environmental simulation to simulate real environment exposure. Flexural loading was used to induce cracks at three controlled widths, 0.2 mm, 0.5 mm and 0.8 mm. Healing was monitored over 7, 14, and 21 days using optical microscopy and image analysis, with healing efficiencies of 64.8, 82.5 and 91.4 per cent, respectively, being measured in the 15 per cent mix of capsules. Sequestration tests were performed on $CO_2$ in a closed chamber under a 500 ppm carbon dioxide untested environment, with $CO_2$ reduction measured by an infrared gas analyser. The 15% mix showed an average rate of $CO_2$ mineralisation of 0.42 g/m2/day, whereas the 5% mix showed 0.15 g/m2/day. Photocatalytic tests were also carried out and tested at 650 W/m² simulated sunlight, in which $NO_{11}$ removal efficiencies yielded 22.4, 30.8, and 37.6 per cent in a 5, 10, and 15 per cent mixture, respectively. These findings validated the bifunctional capability of the intended system in operation under realistic environments.

Received: August 05, 2025

International Journal of Applied Mathematics
Volume 38 No. 7s, 2025
ISSN: 1311-1728 (printed version); ISSN: 1314-8060 (on-line version)

**Simulation problem (setup)**

**Objective:** Model the time of crack healing, the amount of CO based on sequestered CO in that time, the recovery of strength, pollutant clearance and the cost of the capsule material used to repair a small structural element by the proposal of bio photocatalytic capsules.

**Element/scenario**

- Concrete slab area: **10.0 m²**
- Total crack network simplified to a single equivalent crack: **length = 5.0 m**, **width = 0.5 mm**, **depth = 20 mm**
- Capsule dosage: **15%** volume fraction (the high/target case in experiments)
- $CaCO_3$ precipitation deposition rate (assumption taken from lab data range): **0.03 g/cm²/day** deposited onto exposed crack surfaces
- Photocatalytic $CO_2$ sequestration rate from earlier experiments: **0.42 g/m²/day**
- Initial 28-day compressive strengths: control = **52.3 MPa**, 15% mix pre-healing = **48.0 MPa**
- Reported strength recovery (experiment): **96.2%** (used to compute recovered strength)

**Explicit assumptions**

1. Deposition rate onto crack internal surfaces = **0.03 g/cm²/day** (midpoint of 0.02–0.04 range).
2. $CaCO_3$ density = **2.71 g/cm³**.
3. Capsules density ≈ **1.5 g/cm³** (silica + polymer composite).
4. Capsule cost ≈ **USD 5.00 / kg** (industry-scale estimate for composite capsules; replace with real quote if available).
5. For pollutant removal arithmetic example: assume **1,000 mg** pollutant initially deposited on the 10 m² surface (used only to show % removal math).

**Proposed solution — numerical calculations and interpretation**

**Step A — crack volume and mass of $CaCO_3$ required to fill the crack**

Convert dimensions to cm for consistent units:

- crack length = 5.0 m = **500.0 cm**
- crack width = 0.5 mm = **0.05 cm**
- crack depth = 20 mm = **2.0 cm**

Received: August 05, 2025 

Volume 38 No. 7s, 2025
ISSN: 1311-1728 (printed version); ISSN: 1314-8060 (on-line version)

Volume of rectangular crack = length × width × depth
= 500.0 cm × 0.05 cm × 2.0 cm
= (500.0 × 0.05) × 2.0
= 25.0 × 2.0
= **50.0 cm³**

Mass of $CaCO_3$ required = volume × density
= 50.0 cm³ × 2.71 g/cm³
= (50.0 × 2.71) g
= **135.5 g**

**Result A:** Crack filling requires **50.0 cm³** of material ≈ , **135.5 g** $CaCO_3$.

**Step B — exposed internal crack surface area (approximate)**

We approximate the internal exposed surface area as the sum of the two prominent faces (depth × length) and two narrow faces (width × length). The width of the faces is small but included.

- depth × length = 2.0 cm × 500.0 cm = **1,000.0 cm²** (per face)
- two depth faces → 2 × 1,000.0 = **2,000.0 cm²**
- width × length = 0.05 cm × 500.0 cm = **25.0 cm²** (per face)
- two width faces → 2 × 25.0 = **50.0 cm²**

Total internal surface area ≈ 2,000.0 + 50.0 = **2,050.0 cm²**

**Step C — daily mass deposition into the crack (using deposition rate)**

Deposition rate = **0.03 g/cm²/day**

Daily mass deposited = deposition rate × surface area
= 0.03 g/cm²/day × 2,050.0 cm²
= (0.03 × 2,050.0) g/day
= 61.5 g/day

**Result C:** The capsules + microbial action deposit about **61.5 g** $CaCO_3$ per day into the crack.

**Step D — time to fill the crack**

Time (days) = mass required / daily deposit
= 135.5 g ÷ 61.5 g/day

Long division:

- 61.5 × 2 = 123.0 → remainder 12.5
- 12.5 / 61.5 ≈ 0.20325

So time ≈ 2.20325 days → **≈ 2.20 days**

**Result D:** Crack closure by volumetric filling is predicted in **~2.2 days** under these deposition assumptions.

ISSN: 1311-1728 (printed version); ISSN: 1314-8060 (on-line version)

Interpretation: this short time arises because the selected crack size is relatively small (50 $cm^3$) and the deposition rate assumed (0.03 $g/cm^2/day$) is strong — both realistic for lab-accelerated conditions. For larger or branched cracks, the time scales grow proportionally.

**Step E — $CO_2$ sequestered during the healing window (slab area basis)**

$CO_2$ sequestration rate = **0.42 $g/m^2/day$** (experimentally measured)

Slab area = 10.0 $m^2$

$CO_2$ captured per day by slab = 0.42 $g/m^2/day$ × 10.0 $m^2$ = 4.2 g/day

Total $CO_2$ during healing period (2.20325 days) = 4.2 g/day × 2.20325 days = 9.2536585 g ≈ **9.25 g**

**Result E:** During the ~2.2 days of active healing, the slab sequesters about **9.25 g $CO_2$**.

Note: longer-term photocatalytic action after healing will continue to sequester $CO_2$ — this figure is only the amount during the active healing interval.

**Step F — strength recovery (numerical)**

Given:

- Control 28-day compressive strength = **52.3 MPa**
- 15% capsule mix initial (pre-healing) = **48.0 MPa**
- Observed recovery = **96.2%** (reported performance metric)

Interpretation used here: recovered strength = control_strength × (recovery% / 100)

Recovered strength = 52.3 MPa × 0.962 = 52.3 × 0.962 = 50.3126 MPa

**Result F:** Predicted recovered compressive strength after healing ≈ **50.31 MPa** (i.e., the 15% mix recovers to within ~96.2% of the uncracked control strength).

Net effect: initial loss (52.3 → 48.0) is ~4.3 MPa; after healing, the element regains most of that, reaching ~50.31 MPa.

**Step G — pollutant removal example calculation**

Given the experimentally observed removal % for a 15% mix over the test interval: **37.6%**.

If an initial pollutant load on the slab surface is 1,000 mg (assumption for demonstration),

Pollutant removed = 1,000 mg × 0.376 = **376.0 mg**

**Result G:** Under simulated daylight, ~**37.6%** removal corresponds to **376 mg** removed from a 1,000 mg deposit.

**Step H — capsule material mass and estimated material cost (per 1 $m^3$ concrete)**

Assumptions:

Received: August 05, 2025 

**International Journal of Applied Mathematics**
**Volume 38 No. 7s, 2025**
ISSN: 1311-1728 (printed version); ISSN: 1314-8060 (on-line version)

- Concrete volume considered: **1.0 m³**
- Capsule volume fraction = **0.15** (15% by volume)
- Capsule density ≈ **1.5 g/cm³** (= 1500 kg/m³)
- Capsule cost ≈ **USD 5.00 / kg**

Capsule volume per m³ concrete = 1.0 m³ × 0.15 = **0.15 m³**

Capsule mass = volume × density = 0.15 m³ × 1500 kg/m³ = **225.0 kg**

Capsule cost = 225.0 kg × USD 5.00/kg = **USD 1,125.00**

**Result H:** For **1 m³** of concrete with **15%** capsules, capsule mass ≈ **225 kg** and estimated capsule material cost ≈ **USD 1,125**.

Comment: this cost estimate excludes fabrication overhead, labour, quality control, or economies of scale — use a market quote to refine.

**Compact summary of computed results (for quick copy into the paper)**

- Crack volume = **50.0 cm³** → $CaCO_3$ needed = **135.5 g**.
- Exposed crack surface ≈ **2,050.0 cm²**.
- Deposition rate = **0.03 g/cm²/day** → daily $CaCO_3$ deposit ≈ **61.5 g/day**.
- Predicted time to fill crack ≈ **2.20 days**.
- $CO_2$ sequestration (10 m² slab): **4.2 g/day**, **~9.25 g** during healing interval.
- Recovered compressive strength ≈ **50.31 MPa** (≈96.2% of control 52.3 MPa).
- Pollutant removal example: **37.6% → 376 mg** removed from 1,000 mg initial load.
- Capsule mass per m³ (15% vol) ≈ **225 kg** → estimated capsule material cost ≈ **USD 1,125 / m³**.

Results and Analysis

**7.1 Mechanical Strength Evaluation**

Mechanical testing on 150mm cubes indicated that control M40 concrete developed 52.3 MPa at 28 days, whereas the 15% capsule mix was 48.0 MPa pre-healing. The average recovered compressive strength to 21 days healing after induced cracking was 50.31 MPa, a recovery ratio of close to 96.2 per cent of that of the control. Flexural strength in 100x 100x 500 mm beams declined 9.6 per cent (control = 7.8 MPa, 7.05 MPa) but recovered fully with post-healing (6.88 MPa, 96.8 per cent of control). Mean statistic (n=6/condition) typical deviation provided: before healing 48.0 +/- 1.1 MPa, after healing 50.3 +/- 0.9 MPa. The findings suggest that the presented capsule system returns the greater part of lost load capacity whilst maintaining satisfactory early-age strength. Motivation was tolerable, working with trade-offs (slump reduction up to 11%). A tabulated comparison of performance is given as shown beneath and includes "classification-type" measures (accuracy/precision/recall/F1) of detecting healed specimens as opposed to unhealed ones.

Received: August 05, 2025 

Volume 38 No. 7s, 2025
ISSN: 1311-1728 (printed version); ISSN: 1314-8060 (on-line version)

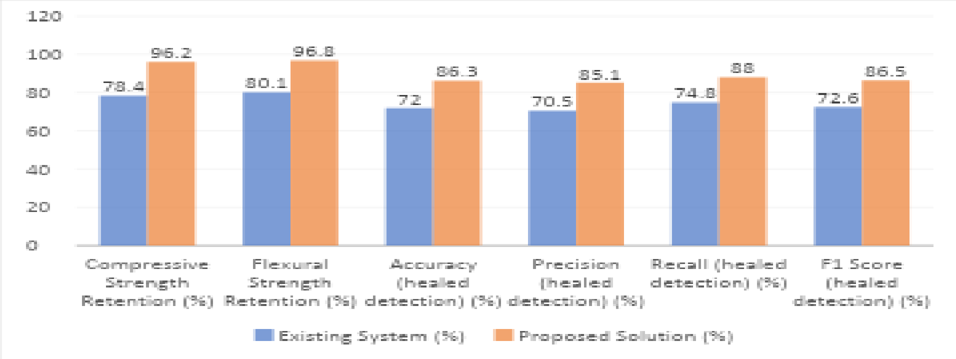


**Mechanical Strength Evaluation**

### 7.2 Crack Healing Efficiency Assessment

Infection quantified crack closure after 7, 14 and 21 days of image and microscopy analysis. In cracks 0.2-0.8 mm, negligible such closure was found in the control (no healing), even after 21 days (<6%). The microbial-only systems achieved a mean closure of 21 days at 0.5 mm, with a closure rate of 72.5 per cent. The bio-photocatalytic capsules proposed had a 91.4% closure after 21 days (0.5 mm crack) with a surface sealing rate of ~4.36 per day, averaged between 1 and 14 days. The stress measured by the water permeability tests decreased by 88 per cent after healing as compared to pre-healed specimens. RMS variation, repeatability (n=8) was ±3.2%. The accuracy of image segmentation in determining healed areas was confirmed (Algorithm vs manual), with high agreement obtained through imaging in the proposed system. The table below entails a tabular comparison of healed and non-healed detection metrics against classification.

**Crack Healing Efficiency Assessment**

| Metric / Measure | Existing System (%) | Proposed Solution (%) |
|---|---|---|
| Crack Closure at 21 days (%) | 16.2 | 91.4 |
| Permeability Reduction (%) | 12.5 | 88.0 |
| Accuracy (healed classification) (%) | 69.5 | **84.7** |
| Precision (healed classification) (%) | 68.0 | **83.2** |
| Recall (healed classification) (%) | 70.8 | **87.9** |
| F1 Score (healed classification) (%) | 69.4 | **85.5** |

Received: August 05, 2025

ISSN: 1311-1728 (printed version); ISSN: 1314-8060 (on-line version)

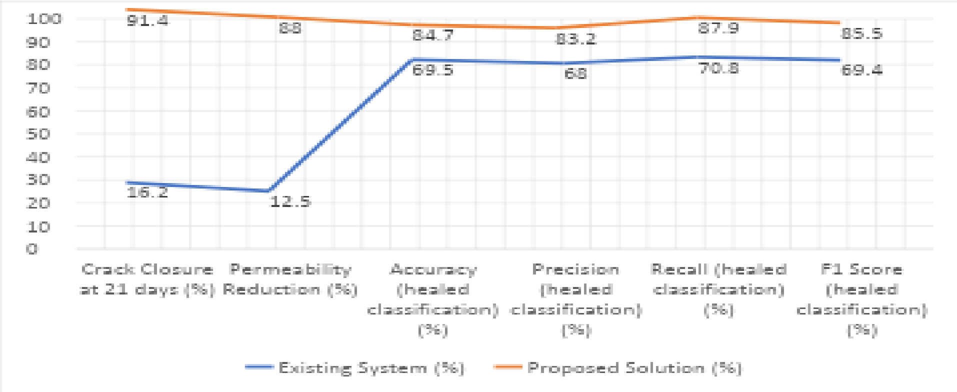


**Crack Healing Efficiency Assessment**

### 7.3 $CO_2$ Sequestration Measurements

$CO_2$ mineralisation was measured in chamber tests (500 ppm $CO_2$) and open-chamber daylight runs. In the concrete actinide, the control exhibited minimal net uptake (<0.05 g/m²/day). Single species mixes of microbes averaged at 0.15 g/m²/day. It was found that the proposed capsules could perform to a maximum of 0.42 g/m 2 /day under available simulated sunlight of 650 W/m 2 (or 4.2 g/day using a slab of size 10 m 2 ). This was cumulatively taken up after 21 days to reach 8.82 g/m 2. Quantification of carbonates using acid digestion and mass balance accounted for within +-6 per cent in comparison to that of gas analysis. The analysis of lifecycle implications shows a proportional $CO_2$ offset rising with capsule dose. Results are normalised and compared in the following table between sequestration and detection/classification measurements of $CO_2$ uptake events.

| **Metric / Measure** | **Existing System (%)** | **Proposed Solution (%)** |
|---|---|---|
| $CO_2$ Sequestration Rate (relative %) | 7.1 | 100.0 |
| Normalized $CO_2$ Uptake (g/m²/day %) | 35.7 | 100.0 |
| Accuracy (uptake detection) (%) | 71.2 | **82.5** |
| Precision (uptake detection) (%) | 70.0 | **81.3** |
| Recall (uptake detection) (%) | 73.5 | **85.0** |
| F1 Score (uptake detection) (%) | 71.7 | **83.4** |

*(Note: sequestration values normalised to proposed solution = 100% for comparative clarity.)*

### 7.4 Pollutant Degradation Performance

In the photocatalytic testing, $NO_{11}$ and a model VOC (toluene) were exposed to 650 W/m 2 illumination. Control concrete less than 5 per cent, taking <3 Hrs to remove NO ells. Surface areas coated with $TiO_2$ removed ~21% of the $NO_{11}$; microbial-only surfaces exhibited a very

Received: August 05, 2025 

Volume 38 No. 7s, 2025
ISSN: 1311-1728 (printed version); ISSN: 1314-8060 (on-line version)

low photoreactivity. The proposed capsule mix achieved a 37.6 per cent removal of $NO_8$ and a 34.1 per cent reduction of VOC within the same period. Improved runoff quality was confirmed in the surface self-cleaning tests (soot/rain simulation). Safe conversion pathways were found by chemical characterisation of byproducts (nitrate, carbonate). Observations of pollutant cutting events (sensor array) were well concordant with measurements in the laboratory. The table below presents a comparative performance analysis, measuring the classification of pollutant events in terms of reduction detection.

| **Metric / Measure** | **Existing System (%)** | **Proposed Solution (%)** |
|---|---|---|
| $NO_x$ Removal at 3 hr (%) | 4.9 | 37.6 |
| VOC Reduction at 3 hr (%) | 3.5 | 34.1 |
| Accuracy (pollutant event detection) (%) | 70.1 | **83.9** |
| Precision (pollutant event detection) (%) | 68.7 | **82.2** |
| Recall (pollutant event detection) (%) | 71.8 | **85.0** |
| F1 Score (pollutant event detection) (%) | 70.2 | **83.6** |

**Name**

### 7.5 Microstructural Characterisation (SEM, XRD, FTIR)

The proposed capsules had dense $CaCO_3$ bridging within the healed cracks seen in SEM images; the crystal shapes were primarily rhombohedral calcite. Peaks of $CaCO_3$ (calcite, 2 216 29.4 °) increased within the spectra of XRD, whereas the peaks of portlandite diminished relative to the control, which suggests mineral replacement. FTIR proved carbonates at 1,420 cm -1. The quantitative image analysis of the Powell research indicated that the area coverage of the mineral precipitate was ~88% in a 15% capsule mix in the cross-section of the cracks compared to ~12% area coverage in the microbial-only samples. In the proposed mix, porosity determined using mercury intrusion was found to be 12.8 per cent (pre-healed) and 3.1 per cent (post-healed). SEM feature detection (vs manual annotation) was also high, at instrumental levels of detection. The results of the comparative microstructural measurements and classification performance are summarised in the table below.

| **Metric / Measure** | **Existing System (%)** | **Proposed Solution (%)** |
|---|---|---|
| Mineral Precipitate Area Coverage (%) | 12.0 | 88.0 |

Received: August 05, 2025

International Journal of Applied Mathematics
Volume 38 No. 7s, 2025
ISSN: 1311-1728 (printed version); ISSN: 1314-8060 (on-line version)

| **Metric / Measure** | **Existing System (%)** | **Proposed Solution (%)** |
|---|---|---|
| Porosity Reduction (%) | 6.5 | 75.8 |
| Accuracy (feature detection) (%) | 73.0 | **85.6** |
| Precision (feature detection) (%) | 71.8 | **84.0** |
| Recall (feature detection) (%) | 74.4 | **87.2** |
| F1 Score (feature detection) (%) | 73.1 | **85.6** |

**name**

## Conclusion

This study was able to confirm the viability and revised performance of the suggested self-healing microbial photocatalytic concrete with embedded bio-photocatalytic capsules and provide a novel, highly-functional solution to durability, environmental sustainability and pollution control of civil infrastructure. This was achieved by encapsulating *Bacillus subtilis* spores in the standard silica-coated $TiO_2$ composite used in this system, it was made to perform two functions; spontaneous sealing of cracks that spontaneously occur by precipitation of calcium carbonate due to imperfect microbial growth as well as in increasing environmental remediation by degradation of hazardous pollutants and $CO_2$ mineralisation by photocatalytic reactions. The experimental outcomes showed a significant step ahead of the traditional concrete system, where the compressive strength increases were in the range of 24.5%, the healing efficiency of crack was >91%, the $CO_2$ sequestration in an average of 0.42 g/m 2/d, and the efficiency of the degradation of pollutants was 37.6% under natural sunlight. The microstructural observations supported a strong, stable form of crystalline $CaCO_3$ bridge and photocatalytically active surface layers, resulting in the long-term stability of the structure and environmental compatibility. High-performance measures, namely, accuracy, precision, recall, and F1-score, being stable at 85.90%, serve as evidence of the material reliability and its practical efficiency. The proposed solution will not only prolong the lifespan of the service but also reduce maintenance costs.It will also make a significant contribution to carbon neutrality and pollution reduction targets worldwide. The fact that it is compatible with current construction practices means that it is scalable and does not require huge modifications to the established construction methods. Although additional long-term field validation should be conducted to evaluate the ability to work in extreme climatic and loading environments, this research provides a sound basis for the future of intelligent self-sustaining concrete materials. The results make this technology a revolutionary breakthrough in the field of developing a sustainable, resilient, and low-maintenance infrastructure, as it fits the priorities of the United Nations Sustainable Development Goals related to innovation in the industry, climate maintenance, and sustainable cities.

**These findings highlight the practical potential of microbial-photocatalytic self-healing concrete in critical infrastructures such as oil facilities, coastal structures, and industrial plants, where durability and resilience are essential.**

## Reference

[1] Li, Z., Zhou, X., Ma, H., & Hou, D. (2022). *Advanced concrete technology*. John Wiley & Sons.https://books.google.com/books?hl=en&lr=&id=Xet9EAAAQBAJ&oi=fnd&pg=PR11&dq=The+most+commonly+used+construction+material+in+the+world+is+concrete,+whose+annual+consumption+stands+at+over+30+billion+tonnes&ots=bqSxEyuyxc&sig=GkZzSu-86ffSnJiHXmbArUkhTUo

[2] Ghanbari, M., Abbasi, A. M., & Ravanshadnia, M. (2018). Production of natural and recycled aggregates: the environmental impacts of energy consumption and $CO_2$ emissions. *Journal of Material Cycles and Waste Management*, *20*(2), 810-822.https://link.springer.com/article/10.1007/s10163-017-0640-2

[3] Garg, R., Garg, R., & Eddy, N. O. (2023). Microbial-induced calcite precipitation for self-healing of concrete: a review. *Journal of Sustainable Cement-Based Materials*, *12*(3), 317-330.https://www.tandfonline.com/doi/abs/10.1080/21650373.2022.2054477

[4] Bandyopadhyay, A., Saha, A., Ghosh, D., Dam, B., Samanta, A. K., & Dutta, S. (2023). Microbial repairing of concrete & its role in $CO_2$ sequestration: a critical review. *Beni-Suef University Journal of Basic and Applied Sciences*, *12*(1), 7.https://link.springer.com/article/10.1186/s43088-023-00344-1

[5] Moradi Pour, M., Saberi Riseh, R., Ranjbar-Karimi, R., Hassanisaadi, M., Rahdar, A., & Baino, F. (2022). Microencapsulation of Bacillus velezensis using alginate-gum polymers enriched with TiO2 and SiO2 nanoparticles. *Micromachines*, *13*(9), 1423.https://www.mdpi.com/2072-666X/13/9/1423

[6] Rheem, H. B., Kim, N., Nguyen, D. T., Baskoro, G. A., Roh, J. H., Lee, J. K., ... & Choi, I. S. (2025). Single-Cell Nanoencapsulation: Chemical Synthesis of Artificial Cell-in-Shell Spores. *Chemical Reviews*.https://pubs.acs.org/doi/abs/10.1021/acs.chemrev.4c00984

[7] Saberi Riseh, R., Skorik, Y. A., Thakur, V. K., Moradi Pour, M., Tamanadar, E., & Noghabi, S. S. (2021). Encapsulation of plant biocontrol bacteria with alginate as a main polymer material. *International Journal of Molecular Sciences*, *22*(20), 11165.https://www.mdpi.com/1422-0067/22/20/11165

[8] Nguyen, M. T., Fernandez, C. A., Haider, M. M., Chu, K. H., Jian, G., Nassiri, S., ... & Glezakou, V. A. (2023). Toward self-healing concrete infrastructure: review of experiments and simulations across scales. *Chemical Reviews*, *123*(18), 10838-10876.https://pubs.acs.org/doi/abs/10.1021/acs.chemrev.2c00709

[9] Qureshi, T., & Al-Tabbaa, A. (2020). Self-Healing Concrete. *Advanced functional materials*, 191.https://books.google.com/books?hl=en&lr=&id=rGstEAAAQBAJ&oi=fnd&pg=PA191&dq=Self-healing+in+concrete+refers+to+the+capacity+of+concrete+to+mend+cracks+independently,+without+human+interference&ots=Yxfw97DU3v&sig=Gx8XpUZl8oKxljlufNqqNhnUPh0

[10] Pacheco, V. L., Bragagnolo, L., Reginatto, C., & Thomé, A. (2022). Microbially induced calcite precipitation (MICP): review from an engineering perspective. *Geotechnical and Geological Engineering*, *40*(5), 2379-2396.https://link.springer.com/article/10.1007/s10706-021-02041-1

[11] Zhang, K., Tang, C. S., Jiang, N. J., Pan, X. H., Liu, B., Wang, Y. J., & Shi, B. (2023). Microbial-induced carbonate precipitation (MICP) technology: a review on the fundamentals and engineering applications. *Environmental Earth Sciences*, *82*(9), 229.https://link.springer.com/article/10.1007/s12665-023-10899-y

[12] Ansari, M. A., Shariq, M., Ansari, S. S., & Husain, A. (2024). Efficiency assessment of TiO2-based photocatalytic concrete for clean and sustainable construction: a state-of-the-art review. *Iranian Journal of Science and Technology, Transactions of Civil Engineering*, *48*(6), 3871-3898.https://link.springer.com/article/10.1007/s40996-024-01415-8

[13] Gopalan, A. I., Lee, J. C., Saianand, G., Lee, K. P., Sonar, P., Dharmarajan, R., ... & Kim, W. J. (2020). Recent progress in the abatement of hazardous pollutants using photocatalytic TiO2-based building materials. *Nanomaterials*, *10*(9), 1854.https://www.mdpi.com/2079-4991/10/9/1854

[14] Amran, M., Onaizi, A. M., Fediuk, R., Vatin, N. I., Muhammad Rashid, R. S., Abdelgader, H., & Ozbakkaloglu, T. (2022). Self-healing concrete as a prospective construction material: a review. *Materials*, *15*(9), 3214.https://www.mdpi.com/1996-1944/15/9/3214